A Model of the Sequential Bending Process for Manufacturing Simulation

D. E. Hardt

E. Constantine

A. Wright

Laboratory for Manufacturing and Productivity,
MIT,
Cambridge, MA 02139

The process of sequential bending has many applications, but the most common is for developing cylindrical shapes from plate. The objective of this work is to develop a process model for use in simulation of the manufacturing of such objects, to provide design sensitivity information, and to explore the potential for improved process control. The process is modeled here as a series of overlapping two-dimensional three-point bends, where the overlap includes the plastic zone from previous bends. This deformed zone is modeled both as a non-flat initial geometry for the next bend and as a locally strain-hardened material with residual stresses. For process simulation the model is incorporated into a measurement and control simulation that allows either operator-controlled algorithms or automatic control to be employed. A series of experiments were performed on plates of steel, aluminum, and brass to examine the accuracy of the model. Good agreement was found, but only after adjusting the assumed material parameters. Results show that the prior bending history has a marked effect on the basic process resolution, and therefore on the effective precision and sensitivity of the process.

Introduction

This research was initiated to develop manufacturing process simulation for the purpose of improving product design. The basic goal is to provide detailed manufacturing information to the product designer at an early stage, to permit optimal material and process selection (MAPS). The subject process, sequential bending, was chosen because of its importance to the shipbuilding industry and because of the need to explore a means for "precision fabrication" whereby the ultimate precision limits for formed and welded structures can be determined.

More specifically, the model developed here is intended to capture the essential mechanics of the sequential bending process so that process inputs (such as machine geometry and displacement) could be related to the geometry outputs of curvature and residual stresses through a set of process parameters (including material parameters and machine geometry). Such a *process model* is shown schematically in Fig. 1(*a*). However, to simulate the actual operation of this process in a realistic manufacturing context requires that the shop level control applied to the process (either operator algorithms, quality control driven means, or real-time process control) be included as well. Accordingly, *process simulation* is developed by the addition of some type of part measurement and attendant control system as shown in Fig. 1(*b*).

Using such a model and simulation, the designer can subject a particular material and geometry design to a thorough manufacturing simulation, including exploration of feasible processing conditions, process optimization via parameter sensitivity analysis, and finally simulation of the "effort" or "cost" required to achieve a specified tolerance given the process and the expected uncertainty in material and machine properties. The application of this simulation to such a task is covered in Hardt et al. (1989) in the context of shipbuilding.

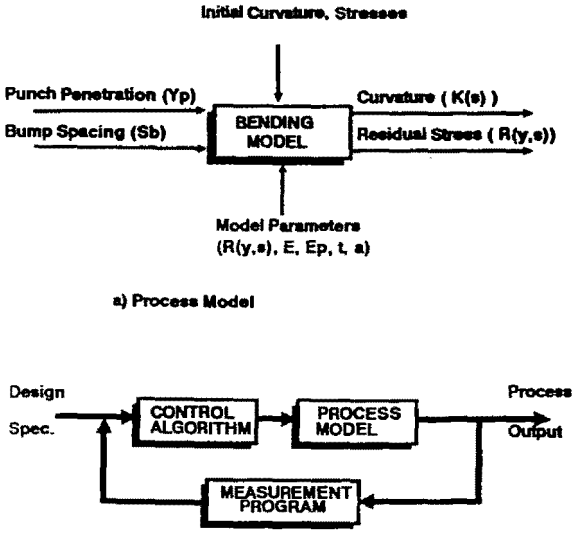

Fig. 1 Process model and process simulation scheme

Contributed by the Production Engineering Division for publication in the JOURNAL OF ENGINEERING FOR INDUSTRY. Manuscript receivted September 1989.

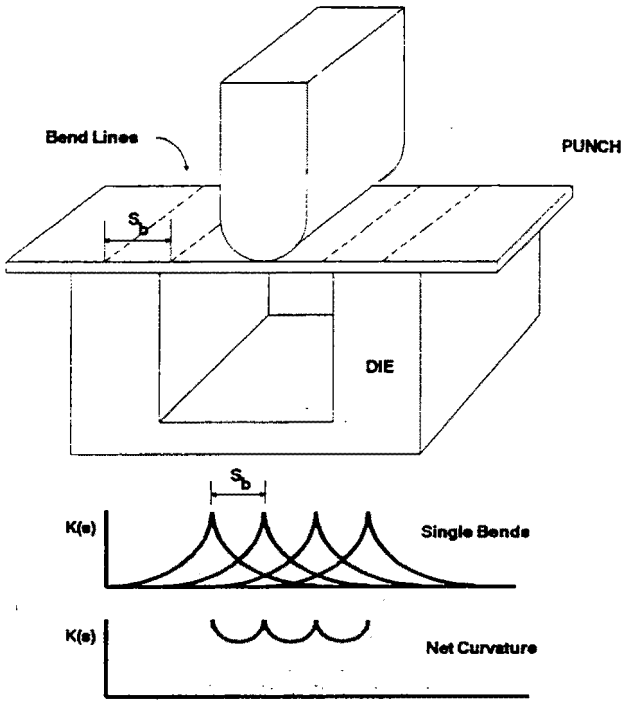

Fig. 2 Sequential bending

Background

The basic process of sequential bending involves creating a series of three-point bends in a sheet or plate that is incremented to develop parallel bend-lines and overlapping curvature changes in the part, as shown in Fig. 2. As shown in the figure, the key modeling issues are determination of the effect of each local three-point bend, and the cumulative effect of overlapping bends. While the mechanics of simple bending have been thoroughly explored, both analytically (e.g., Queener et al., 1968, and Sidebottom and Gebhardt, 1979) and using numerical methods (Oh and Kobayashi, 1979), the details of overlapping sequential bending have not. Sequential bending was addressed by Hardt and Chen (1985) for non-constant thickness plate, but only in the context of real-time control, and the process model presented there was incomplete with respect to the present discussion.

The area of process simulation has received some attention in recent years, often under the heading of Computer Aided Engineering (CAE). For example, Subramanian et al. (1977) have developed extensive process simulation for forging for the express purpose of tooling and preform design. While the emphasis is on *process design*, the basic model and simulation are equally applicable to *product design*. Maddux and Jain (1986) have developed several manufacturing process simulations that help illustrate the mechanical effects of these processes on the product. More recently, the process of sand casting has received modeling attention, particularly with respect to thermal analysis for shrinkage and void formation (Berry et al., 1989).

All of the above efforts provide excellent *models* for the respective processes, but none have yet developed the process operation simulation as defined above. This research provides both the specific process models for sequential bending and the simulation context to permit thorough design exploration. Design topics of particular interest include simulation of various process measurement and control options and simulation of the development of tolerances, for which there appears to be no previous work.

Model Development

Sequential bending is most frequently performed on a press brake, using tooling with large nose radii as shown in Fig. 2. The part is aligned along the current bend line, and a bend (typically of low magnitude, and consequently large springback) is made. The part is then incremented to the next bend line and the same bend performed on this new location. Details of operation vary from shop to shop, but a typical procedure involves bending with a specified punch penetration (Y_p) and bend line spacing (s_B) for the entire arc-length of the bend. The part is then measured, and the bending repeated, either by changing Y_p or s_b, until the desired part radius is achieved.

For this process, then, the inputs are the Y_p and s_b, and the output is the *unloaded* curvature along the part arc-length $K_u(s)$, as well as the residual stresses in the cross section. However, for most applications the geometry outputs are expressed in terms of the average part radius R_{ave} and the radial or circularity error e_R. The functional relationship between these inputs and outputs is governed by the following process parameters:

Material Properties
- modulus E
- yield strength σ_y
- plastic modulus E_p

Material Geometry
- thickness t
- initial curvature $K_i(s)$
- width

Boundary/Machine Conditions
- die width
- die nose radius
- punch radius
- machine stiffness
- punch positioning accuracy

Since the input-output relationship will strongly depend on these parameters, and several are subject to considerable variation (such as σ_y, t and $K_i(s)$), it is clear that even with a highly accurate predictive process model, some form of feedback control will be required to achieve a specific part radius in normal production.

The kernel of the sequential bending model is a three-point bending analysis. While the mechanics of this process are straightforward, the use in an overlapping bend model requires that the model account for non-flat initial geometry, residual stress, and strain-hardening of the overlapping material.

The basic three-point bending solution proceeds as follows: Given the stress-strain (σ–ϵ) relationship for the material, the moment curvature relationship (M–K) is found by integration over the cross section:

$$M = \delta K EI \qquad K < K_Y$$

$$M = \int_0^{t/2} \sigma(\epsilon) y w dy \qquad K \geq K_Y \tag{1}$$

Where:

$\delta K = K - K_{initial}$

$\epsilon = \delta K y$

I = area moment of inertia

y = distance from the neutral axis

w = part width

K_Y = yield curvature

Equation (1) permits any stress-strain relationship to be used (analytical or discrete data), and is particularly useful when strain hardening occurs during the process. Notice also that it does not assume that the initial curvature is zero. In the actual

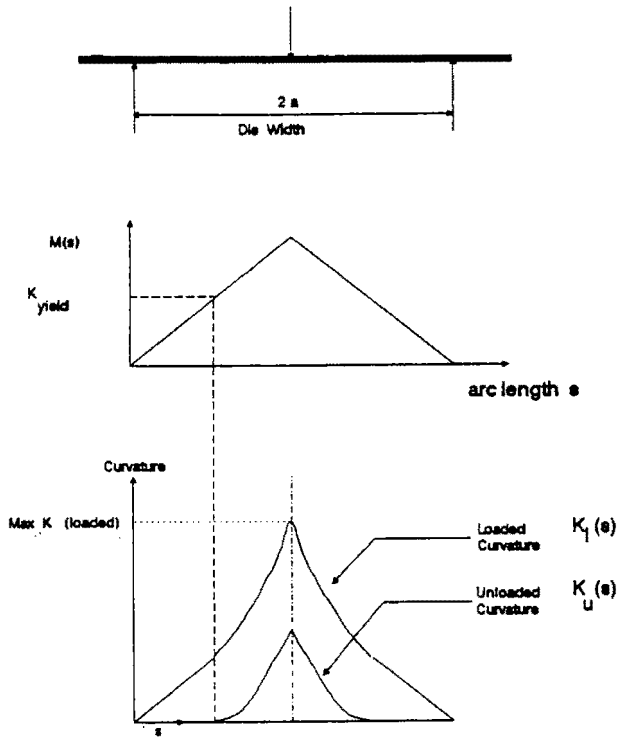

Fig. 3 Moment curvature relationships for three-point bending

implementation of the model, the moment-curvature relationship is recomputed for each bend and for each location along the arc-length of the part. In this way the effect of both previous shape changes (K_i) and previous working (which will affect the stress-strain relationship) can be accounted for. (For all uses of the model herein, a linear strain-hardening model with plastic modulus E_p is used.)

Given this M–K relationship, the first step in the solution is to determine the curvature distribution over the loaded arc length. Accordingly, a moment is assumed that is symmetrical and linear with s (see Fig. 3), and it is specified completely given the total arc-length s_T and the maximum moment M_{max}. Thus:

$$M(s) = M_{max}(2s/s_T) \qquad s < 1/2s_T$$
$$M(s) = M_{max}(1 - 2s/s_T) \qquad s > 1/2s_T \tag{2}$$

The loaded curvature distribution for the bend $K_l(s)$ can be found by inverting Eq. (1) and using Eq. (2) as the input:

$$K_l(s) = K(M(s))$$

Since M–K will in general not be an analytical expression, thus not invertible, this calculation must be performed iteratively.

The general shape of $K_l(s)$ is shown in Fig. 3. It can be seen that the region near the edge, where the moment is below yield, remains linear with arc-length. However, near the center, as the material yields, the curvature increases nonlinearly with moment, leading to the concave curve with a peak under the punch. When the part is released, the net moment on the section must vanish and the part will "spring back." This is analogous to applying a negative moment equal to the originally applied moment. Assuming at present that the negative moment is entirely elastic, the net effect is to completely flatten the elastic regions of the $K_l(s)$ curve, and to reduce the peak curvature of the unloaded section (see Fig. 3). Thus, the unloaded shape ($K_u(s)$) is found from:

$$K_u(s) = K_l(s) - M(s)/EI \qquad K_l(s) \geq K_Y$$
$$K_u(s) = 0 \qquad K_l(s) < K_Y \tag{3}$$

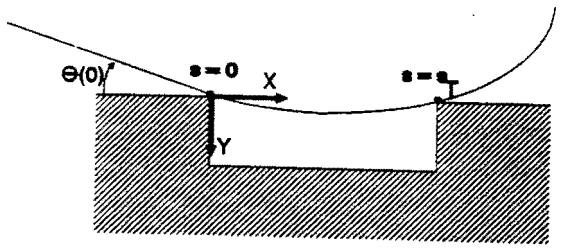

Fig. 4 Bending geometry

If, because of non-zero initial curvature or residual stresses, the unloading moment causes *plastic* deformation of the material, the unloaded curvature pattern will deviate from this ideal. This modification has been incorporated in this model by carrying initial stress as a function of y along with all calculations, and recalculating M–K from Eq. (1) with each bend.

Notice that the above calculation requires both an assumed moment distribution and magnitude M_{max}. However, the process input is Y_p, and at this point the *actual* punch penetration that would cause the assumed bending moment must be determined. This can be calculated from the deformed part geometry, shown in Fig. 4. From $K_u(s)$, the shape of the part in Cartesian coordinates can be found from the following:

$$\Theta(s) = \int_0^{s_T} K(s)ds + \Theta(0)$$
$$dY(s) = \sin(\Theta + d\Theta)ds$$
$$dX(s) = \cos(\Theta + d\Theta)ds$$
$$d\Theta(s) = K(s)ds \tag{4}$$

where $\Theta(0)$, the angle of the plate at the left hand side of the die, is found iteratively on the basis of contact with the right-hand side of the die (see Fig. 4), and $X(0) = Y(0) = 0$.

Given $X(s)$ and $Y(s)$, the punch penetration can be found from:

$$Y_p = Y(s_m) - Y_i(s_m)$$
$$s_m = s \text{ when } X = 1/2 \text{ die width} \tag{5}$$

(Note here that the last assumption implies either a symmetric part or a punch of zero radius.) This penetration is then compared with the specified input penetration and the moment is incremented if the penetration is too small. Owing to the nonlinear nature of the calculations, this iteration is performed without gradients, and moment increments are bisected if the predicted penetration exceeds the input value.

This calculation is performed using $K_l(s)$ since it seeks the penetration when under load. The final *unloaded* shape of the bend is found in a similar manner by substituting $K_u(s)$ into Eq. (4).

The difference between this analysis and other three-point bending approaches is the use of curvature *change* rather than absolute curvature as the model output. Since no *a priori* assumptions are made about the plate curvature before each bend, the model allows consideration of both intentional (sequential bending) and nonintentional initial curvature (e.g., warped stock).

The effect of non-zero initial curvature will be illustrated below, but can be understood heuristically with the help of Fig. 5. Punch penetration Y_p is always referred to a fixed datum. However, the moments generated by Y_p will vary according to the point at which it makes contact with the material. If the material has significant initial curvature, the "effective" punch penetration (and the concomitant bending moment) will be less that if the plate were flat. Since the punch penetration calculated in Eq. (5) is based on the curvature change (as

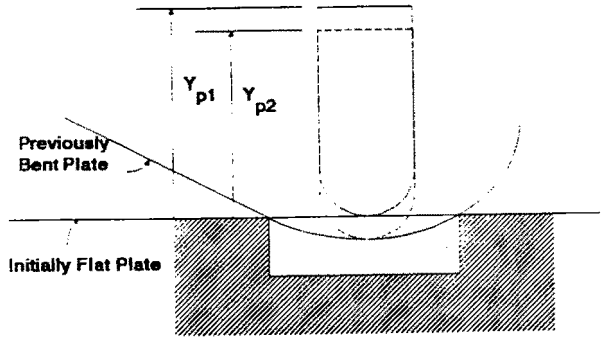

Fig. 5 Effect of initial shape on effective penetration. Note that $Y_{p1} > Y_{p2}$

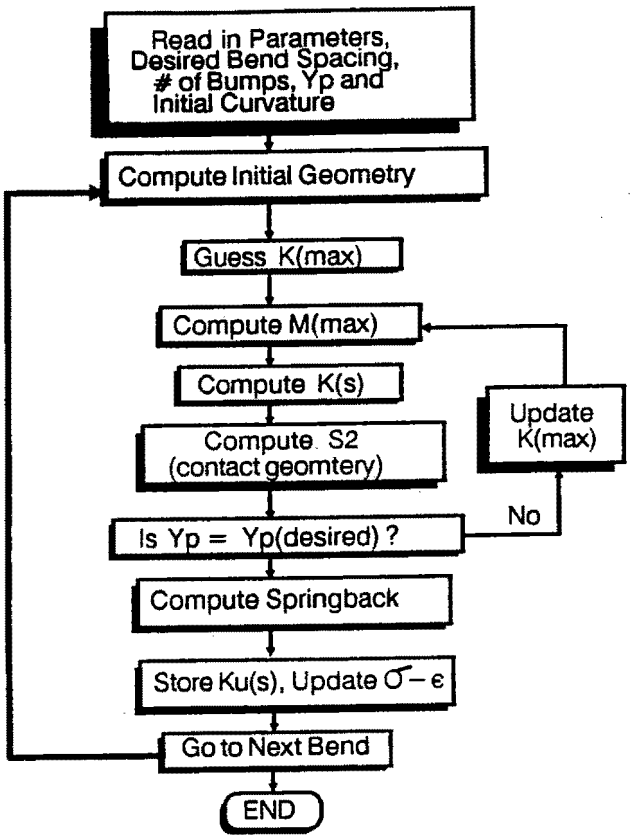

Fig. 6 Flowchart for model calculations

reflected by $Y(s_m)$ and on the initial curvature (as reflected by $Y_i(s_m)$), the Y_p in Eq. (6) correctly reflect this effect.

Sequential Bending. The extension of this model to sequential bending is now straightforward. Once the shape of a single bend has been calculated, the result is $K_u^1(s)$, where $s(0) = 0$. The part is then incremented by the spacing s_b, and the initial curvature for the next bend is given by

$$K_i^2(s) = K_u^1(s - s_b) \tag{6}$$

which serves as the initial curvature for the next bend calculation. Also, the corresponding changes in the interior constitutive relationships for $\sigma\epsilon$ caused by strain hardening and residual stresses are carried along to reflect the initial bend and used in the equation to determine the *local* moment-curvature relationship. The single bend model is then executed again, resulting in a new distribution $K_u^2(s)$. Again the part is incremented by s_b and the model executed. In this way the sequence of bends is simulated and corresponding complete curvature distribution developed. A flowchart for the model calculations is shown in Fig. 6.

This result of this procedure is shown in Fig. 7, where a sequence of five bends of equal penetration and spacing are simulated. From the figure it is evident that the initial bend yields the largest maximum curvature, while the second has the smallest. The third and fourth then approach a steady value. This occurs because the first bend is the only one that sees a flat plate, and the fixed Y_p yields the highest M_{max}. This in turn causes the greatest plate deflection, and decreases the effective penetration of the punch on the second bend, yielding the lowest M_{max} for the sequence. This "undershoot" is then mitigated by the next bend, and the process finally settles into a steady state.

Model Outputs

The fundamental output of the model is $K_u(s)$, as shown in Fig. 7. The output of greatest interest in practice (primarily because of the measurement methods used) is the average radius $R_{ave} = 1/K_{ave}$. In addition, it is often important to know the maximum circularity error R. Circularity errors are calculated by first finding a "best fit" center located by averaging the locations of all the centers found for the X, Y data in the "middle" part of the plate. (This was done by breaking these points into 3 groups, and using perpendicular bisectors of two chords for each center.) Then the average radius can be calculated by taking the average distance that the data points in the X, Y file are from this "average center." The circularity error is obtained by taking each coordinate point in turn and calculating the difference between its distance from this center and the value of average radius.

The model alone can only be used in an "open-loop" fashion, that is a Y_p, s_b input pair is specified, and the corresponding R_{ave} and R calculated based on the assumed model parameters. For example, it is necessary to know all of the model parameters listed above to perform this calculation. For most materials, however, many of these parameters are poorly known. For example, the mil-spec for HY80 (a typical military ship hull material) call for a *minimum* yield point of 80,000 psi, but allow variations as high as 100,000 psi. Likewise, plate thickness must be above a minimum value, but can exceed that minimum by up to 10 percent. Also, the processing history of material can affect the yield and the strain hardening parameter (E_p).

Accordingly, it is important to know what the sensitivity of the outputs are to these variations in these parameters. Since the basic model does not have an analytical solution, such gradients cannot be directly determined. Instead they are determined from successive calculations using fixed input and perturbing the parameter of interest. Typical sensitivities of interest are:

$$\frac{\partial R_{ave}}{\partial \sigma_Y} = \frac{\Delta R_{ave}}{\Delta \sigma_Y}$$

$$\frac{\partial R_{ave}}{\partial t} = \frac{\Delta R_{ave}}{\Delta t}$$

$$\frac{\partial R_{ave}}{\partial E_p} = \frac{\Delta R_{ave}}{\Delta E_p}$$

$$\frac{\partial (\delta R)}{\partial \sigma_Y} = \frac{\Delta (\delta R)}{\Delta \sigma_Y}$$

$$\frac{\partial (\delta R)}{\partial t} = \frac{\Delta (\delta R)}{\Delta t}$$

$$\frac{\partial (\delta R)}{\partial E_p} = \frac{\Delta (\delta R)}{\Delta E_p}$$

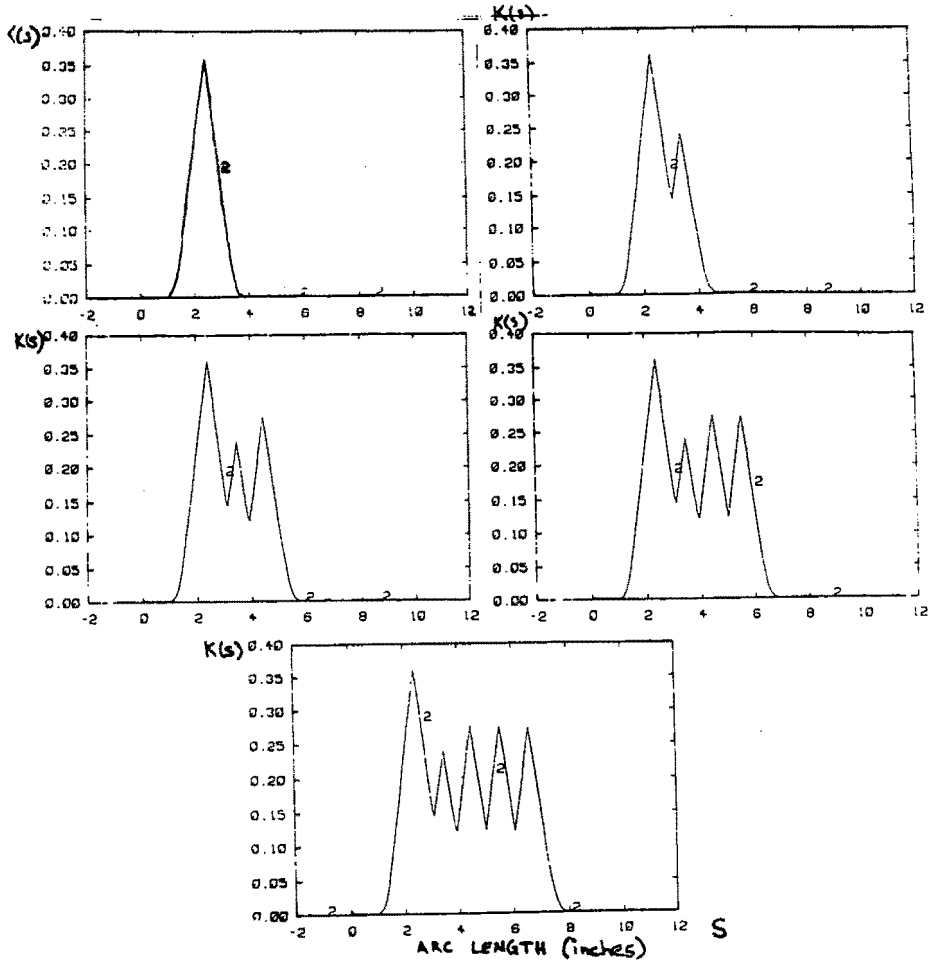

Fig. 7 Curvature distributions

Since this is a highly nonlinear process, these sensitivity functions are themselves dependent upon the operating point of the process. For a given desired R_{ave} and machine geometry, the operating point is defined by combinations of Y_p and s_b that achieve that radius. Figure 8 shows a pair of sensitivity functions plotted as a function of the inputs Y_p and s_b. Also shown in the figure is a set of operating points that will yield constant average radius part. As shown in this figure, the sensitivity functions can be strongly dependent upon the operating point.

Experiments

A series of experiments were performed to examine the use of this model and attendant process simulation and to assess its accuracy. The objective was to form a part of specified radius. The process control used for the experiments involved performing a sequence of bends using constant punch penetration and bend spacing that would intentionally underbend the part. The average radius was then measured, and punch penetration was incremented until the desired radius was reached. (This simulates a production process where a target radius is achieved by working up from intentionally smaller bend radii to avoid overbending.) The radius was measured both by a specially designed coordinate measuring machine having an accuracy of 0.002 in. in all directions, and with radius templates of 1/4 in. radius resolution. Several trials were executed using different starting penetrations and penetration increments.

The tests were performed on a Cincinnati Inc. CB 90 hydraulic pressbrake. For the first set of experiments, the specimens were 6.35 mm (1/4 in.) thick HY 80 steel and were 60 mm (4 in.) wide by 180 mm (12 in.) long. The tooling involved a die of 90 mm (6 in.) width with an edge radius of 6.35 mm (1/4 in.). The punch likewise had a 6.35 mm nose radius.

Since the position system on the brake is designed for good repeatability but has poor absolute accuracy, the punch position was controlled by using positive stops at either end of the brake. These stops contained shims that could be removed in increments of 0.45 mm (0.0156 in.) as needed. Such an approach ensures penetration accuracy, but did not limit the minimum increment in penetration. The following specimens were used:

-4 pcs: Brass (70/30 HH, 18×4×1/4)
-4 pcs: Aluminum (2024-T351, 24×4×1/2)
-2 pcs: Tool Steel (AISI-O1, oil-hardened, 18×4×1/4)

(The latter was precision-ground flat stock used to eliminate initial out of flatness errors.)

The actual thicknesses of these pieces were measured using a micrometer and found to be:

-Brass: 0.253 in. (all pieces from same sheet)
-Aluminum: 0.519 in. (all pieces from same sheet)
-Tool Steel: 0.250 in., 0.252 in.

As discussed earlier, the model is sensitive to material properties. However, the best estimates for these material were found from handbook data (Metals Handbook, 1983), and are listed in Table 1.

The overall procedure followed in all the bending experiments was to choose a particular bump spacing (s_b) for the

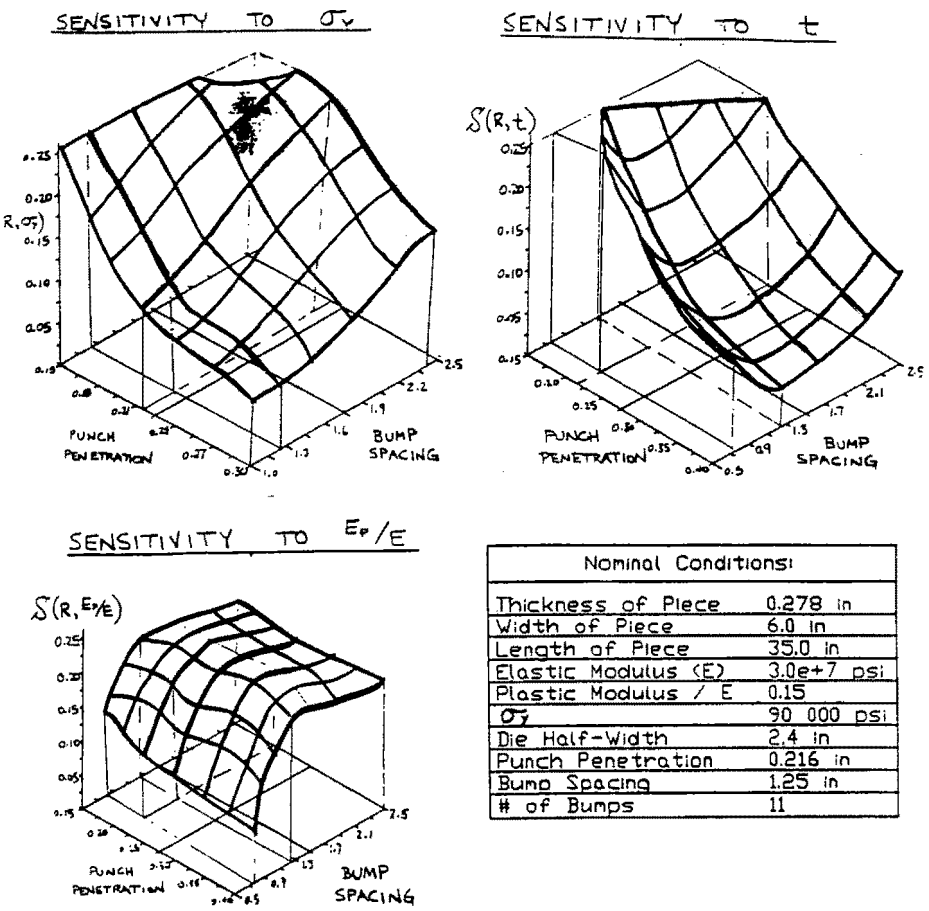

Nominal Conditions:	
Thickness of Piece	0.278 in
Width of Piece	6.0 in
Length of Piece	35.0 in
Elastic Modulus (E)	3.0e+7 psi
Plastic Modulus / E	0.15
σ_Y	90 000 psi
Die Half-Width	2.4 in
Punch Penetration	0.216 in
Bump Spacing	1.25 in
# of Bumps	11

Fig. 8 Sensitivity functions

Table 1 Nominal Material Parameters

	Brass	Aluminum	Tool-Steel
Yield Strength (10^3psi)	52	47	70
Young's Modulus (10^6psi)	16	10	30
Ep/E	0.28	0.43	0.15

piece being bent, and to start out by bending the piece to a radius greater than the desired target radius. In all the experiments, a target radius of 18 inches was used. A "bend" was considered to be the process of punching the plate to a fixed punch penetration (Y_p) at each of 9 or 10 evenly spaced locations along the length of the plate. The resulting bent piece approximated a circular shape. After each bend, the piece was measured using a radius template. The template was generated using Auto Cad and comprising a sequence of concentric arcs at increments of 1/4 in. plotted at full scale. In an effort to quantify the amount of variation one could expect from piece to piece, the same bending history was adhered to for all plates of each material.

The choice of bend line spacing was made using the sensitivity functions discussed above, and searching for the value of s_b that minimized the overall sensitivity of the process. The actual procedure for this "robustness analysis" can be found in Constantine (1989). For all three materials, the value of $s_b = 1.5$ in. was chosen for all three materials. After some preliminary tests on each material, a sequence of bends with progressively increasing values of Y_p was settled upon to yield a final radius near 18 inches. Data for all three materials are shown in Table 2.

While there are some variations, the tests show that if identical thickness coupons are used, the bending results for identical trials are essentially identical, given the 0.25 in. resolution of the template measurement method. Radius measurements derived from the coordinates of the surface of the plates were in agreement with the radius template data, and did not significantly improve the measurement resolution.

Simulation of Experiments

The process simulation was first run using the nominal material property values from Table 1. As shown in Table 3, agreement was good, but it was found subsequently that modifying the value of Ep/E used in the model afforded improved agreement, as shown in the last column of the Table. The value of Ep/E was chosen as the parameter to adjust because it is most likely to be in error. This parameter represents a linear approximation of the plastic deformation region of the stress-strain curve for each material above its yield point. Also, the sensitivity function $\partial R/\partial(E_p/E)$ was computed and found to be of significant magnitude, given the uncertainty of this parameter.

NOTES: Experimental radii shown represent average radii for each material. $-R_{nom}$ is the simulation prediction based on nominal values, R_{adj} is the prediction using the adjusted values of E_p/E:

Brass: Ep/E value changed from 0.281 to 0.364.
Aluminum: EP/E value changed from 0.425 to 0.338.
Steel: Ep/E value changed from 0.150 to 0.250.

Conclusions

A model of the sequential bending process has been developed and integrated into a manufacturing process simulation. This simulation includes the various forms of control that can be applied to achieve a desired degree of precision from the process. The basic model is general with respect to constitutive

relationship for the material and includes all effects of machine and material geometry. A possible extension of this model would be to consider nonconstant material thickness along the arc length of the plate. The model is, however, restricted to two dimensions. Therefore, a reformulation at the expense of simplicity would be required to account for thickness variations along the bend line, for example.

The use of the sensitivity functions, while not the emphasis of this paper, could be one of the most powerful uses of such simulations. By applying process optimization methods, such as those proposed by Taguchi and Wu (1980), a range of operation for least sensitivity to expected variations can be found and specified. In so doing, the designer can exploit the actual precision of the process and examine the effect of in-process control.

The ability of the model and simulation to mimic actual bending was confirmed in a set of experiments on various materials. The experiments also served to emphasize the strong sensitivity of the model output to various material and geometric parameters. However, this potential for error is not onerous in the application of the model and simulation to design, since the object is to determine the basic operating conditions and optimal operating points for the process. The initial focus is on material and process selection, while actually specifying process operation details is of secondary importance.

While the basic mechanics of this process are rather straightforward, the geometric complexity of the sequential bending process, and the attendant sensitivity, illustrate the art required to design for and operate this process. Through models such as those presented here, applied broadly to many manufacturing processes, it is hoped that a more rational basis for process selection and operation can be established.

Table 2 Experimental Data

Piece No.	Bend No.	*Yp*	Average Radius
Brass 01	1	0.170	28.63
	2	0.186	28.38
	3	0.202	25.63
	4	0.233	20.38
	5	0.264	17.38
Brass 02	1	0.170	28.63
	2	0.202	25.63
	3	0.233	20.63
	4	0.264	17.63
Brass 03	1	0.170	28.63
	2	0.202	26.13
	3	0.233	20.88
	4	0.264	17.38
Brass 04	1	0.170	29.13
	2	0.202	26.63
	3	0.233	21.38
	4	0.264	17.63
Aluminum 01	1	0.153	28.76
	2	0.184	26.51
	3	0.215	20.01
	4	0.231	19.26
Aluminum 02	1	0.153	28.76
	2	0.184	25.76
	3	0.215	20.51
	4	0.231	19.01
Aluminum 03	1	0.153	28.76
	2	0.184	26.01
	3	0.215	20.51
	4	0.231	19.26
Aluminum 04	1	0.153	28.76
	2	0.184	25.76
	3	0.215	20.26
	4	0.231	19.26
Steel 01	1	0.167	23.63
	2	0.199	22.13
	3	0.230	18.13
Steel 02	1	0.169	22.13
	2	0.201	21.13
	3	0.232	17.38

Acknowledgments

This work was supported by the Office of Naval Research, under Grants No. N00014-87-K-0462 and N00014-89-J-1187.

References

1 Hardt, D. E., Constantine, E., and Wright, A., 1989, "A Design Oriented Model of Plate Forming for Shipbuilding," *Proc. SNAME Conference*, Arlington, Va., Sept.

2 Queener, C. A., and DeAngelis, R. J., 1968, "Elastic Springback and Residual Stresses In Sheet Metal Formed By Bending," *Trans. of ASME*, pp. 757-768.

3 Hansen, N. E., and Jannerup, O., 1979, "Modeling of Elastic-Plastic Bending of Beams using a Roller Bending Machine," *ASME Journal of Engineering for Industry*, 101, pp. 304-310.

4 Oh, S. I., and Kobayashi, S., 1979, "F. E. M. Analysis of Brake Bending," Final report to Batelle Columbus Labs, Contract No. F33615-77-C-5059, UCAL, Berkeley.

5 Hardt, D. E., and Chen, B. S., 1985 "Control of a Sequential Brake-forming Process," *ASME Journal of Engineering for Industry*, Vol. 107, May.

6 Sidebottom, O. M., and Gebhardt, C. F., 1979, "Elastic Springback in Plates and Beams Formed by Bending," *Experimental Mechanics*, Vol. 19, Oct. pp. 371-377.

7 Subramanian, T. L., Akgerman, N., and Altan, T., 1977, "Computer Aided Preform Design for Precision Isothermal Forging," *Proc. 5th North American Manufacturing Research Conference*, pp. 198-203.

8 Maddux, K. C., and Jain, S. C., 1986, "CAE for the Manufacturing Engineer: The Role of Process Simulation in Concurrent Engineering," *Manufacturing Simulation and Processes*, ASME, PED Vol. 20, 1986, pp. 1-16.

9 Taguchi, G., and Wu, Y., 1980, *Introduction to Off-Line Quality Control*, ASI, Dearborn.

10 Berry, J. T., Hill, J. L., and Stefanescu, D. M., 1989, "Computer Aided Design for Casting and Solidification Technology," *Proc. Advances in Manufacturing Systems, Integration and Processes*, SME, 1989.

11 Anon, 1983, *Metals Handbook*, ASM.

12 Constantine, E., 1989, "A Design-Oriented Process Simulation of Plate Forming," S. M. Thesis, MIT, Oct.

Table 3 Simulation/Experiment Comparisons

	Bend No.	Y_p(in)	R_{expt}	R_{nom}	Error	R_{adj}	$Error_{adj}$
Brass	1	0.170	28.80	25.85	−2.95	28.80	0.00
	2	0.202	26.13	23.16	−2.97	25.25	−0.88
	3	0.233	20.96	19.65	−1.31	21.45	+0.49
	4	0.264	17.55	17.07	−0.48	18.58	+1.03
Aluminum	1	0.153	28.76	32.31	+3.55	28.59	−0.17
	2	0.184	26.01	28.22	+2.21	25.51	−0.50
	3	0.215	20.32	23.80	+3.48	21.44	+1.12
	4	0.231	19.20	21.73	+2.53	19.71	+0.51
Steel	1	0.168	22.88	20.52	−2.36	23.34	+0.46
	2	0.200	21.63	19.56	−2.07	21.49	−0.14
	3	0.231	17.76	16.70	−1.06	18.34	+0.58

NOTES: Experimental radii shown represent average radii for each material. − R_{nom} is the simulation prediction based on nominal values, R_{adj} is the prediction using the adjusted values of E_p/E:

Brass: *Ep/E* value changed from 0.281 to 0.364.
Aluminum: *EP/E* value changed from 0.425 to 0.338.
Steel: *Ep/E* value changed from 0.150 to 0.250.